Journal of
Renewable Energy Research and Applications (RERA)

Vol 1, No 2, 2019, 175-185 *DOI: 10.22044/rera.2020.9282.1023*

Thermodynamic and Exergy Analyses of a Novel Solar-Powered CO_2 Transcritical Power Cycle with Recovery of Cryogenic LNG Using Stirling Engines

A. Naseri[1], M. Fazlikhani[1], M. Sadeghzadeh[2*], A. Naeimi[1], M.Bidi[1*], and S. H. Tabatabaei[2]

1. Faculty of Mechanical and Energy Engineering, Shahid Beheshti University, A.C., Tehran, Iran.
2. Department of Renewable Energy and Environmental Engineering, University of Tehran, Tehran, Iran.

Receive Date 13 January 2020; Revised 2 February 2020; Accepted Date 22 February 2020
**Corresponding authors: milad.sadeghzadeh@gmail.com; m_bidi@sbu.ac.ir (M. Sadeghzadeh and M. Bidi)*

Abstract

In this paper, a novel CO_2 transcritical power cycle, which is driven by solar energy integrated by a cryogenic LNG recovery unit, is investigated. In the proposed cycle, the condenser unit of the CO_2 power cycle is replaced by a Stirling engine. The thermodynamic and exergy analyses are carried out to evaluate the performance of the presented system. Furthermore, in order to investigate the impact of utilization of Stirling engines instead of the conventional condenser units, the proposed cycle is compared with the typical CO_2 power cycle. The results obtained show that employing the Stirling engine decreases the exergy destruction from 17% in the typical cycle to 8.85%. In addition, the total generated power of the novel system is considerably boosted up by about 15 kW in the off-peak times and more than 20 kW in the peak time. Moreover, the integration of the Stirling engine also decreases the LNG mass flow rate. Therefore, the required heat exchanger area in the LNG heater is also lowered.

Keywords: *Solar collector, Transcritical CO_2 power cycle, LNG; Stirling engine, Exergy.*

1. Introduction

Destructive environmental effects of fossil fuel combustion and providing the energy demand of the developing societies are taken into account as the most facing challenging issues [1, 2]. Therefore, many efforts such as the exploitation of renewable energy resources have been made to respond and support the acceptable solutions for these problems [3–5]. Among the renewable sources, solar energy is a vastly available source that has the potential to be employed in solar collectors and considered as a low degree heat source to generate a valuable energy [4, 6, 7]. A CO_2 Rankine cycle can be integrated into a solar source to provide an enhanced level of energy utilization since it is neither toxic, corrosive, and flammable nor explosive, and also have low hazardous ecological impacts [8-10]. Moreover, this application has more favourable thermodynamic advantageous such as being capable of easily achieving the supercritical mode (7.38 MPa and 31.1 ˚C) [11]. In this specific research field, *Chen et al.* [12] have compared the CO_2 supercritical power generation cycle with an organic Rankine cycle and the conventional Rankine cycle, and have demonstrated that it produces a higher output power under the same operational conditions. Chen *et al.* have also performed an evaluation of the hybridization of solar energy to the CO_2 power cycle [13]. *Cayer et al.* [14] have carried out an investigation on using low-grade heat source of process gases to be used in the CO_2 power cycle. In addition, *Wang et al.* [15] have enhanced the performance of a similar system by employing the genetic algorithm (GA) and artificial neural network (ANN). *Zhang et al.* [16–22] have presented a solar-based CO_2 power cycle for co-generation of heat and power, and have studied their model numerically and also performed a measurement on heat transfer specifications of the working fluid. One of the most significant considerations in the CO_2 cycle is to provide a practical heat sink for CO_2 condensation due to the closeness of the CO_2 critical temperature to the ambient temperature. In some research works, the cryogenic liquefied natural gas (LNG) has been considered as the heat sink. *Lin et al.* [23] have used LNG as a heat sink of a modern CO_2 transcritical Rankine cycle. *Song et al.* [24] have performed a thermodynamic investigation on a solar-driven transcritical CO_2 power cycle, employing the condenser heat rejection to an LNG evaporation system. *Zhang* and *Lior* [25] and *Liu et*

al. [26] have recommended using the LNG evaporation unit as the heat sink of a semi-combined cycle of CO_2 Brayton cycle and a supercritical CO_2 Rankine-like cycle. In order to provide a better understanding of the cryogenic energy, various investigations have been performed on the exergy analysis of LNG by employing a Stirling engine to generate electricity. *H. Dong et al.* [27] have studied a Stirling engine with seawater (heat source) and LNG (heat sink), and have evaluated its thermodynamic performance feasibility. Electricity generation has also been assessed by *Szczgiel et al.* [28] and *Szargut et al.* [29] using a cryogenic LNG-based Stirling engine. *Ge et al.* [30] *have* considered a CO_2 transcritical power cycle at a low capacity and have evaluated its performance at different operational conditions. The cycle was composed of a plate thermal coil heater, a turbine, a recuperator, an air-cooled condenser, and a pump. It was reported that the turbine efficiency was not lower than its isentropic efficiency and also the heat source flow rate had a minor influence on the operation of the system. The maximum efficiency of the system was achievable when the system operated at a high pressure before entering into the turbine or in a low-temperature heat source. *Sarmiento et al.* [31] have performed a parametric study on a solar-based transcritical CO_2 power generation cycle. *Alzahrani and Dincer* [32] have studied the hybridization of the concentrated solar system with transcritical CO_2 power cycle and have examined its performance through exergy analysis. *Naseri et al.* [33] have investigated the integration of Stirling engine and solar-based transcritical power generation cycle to produce water and hydrogen. The system was designed to take more benefits from the available exergy stream and to increase the products of the cycle that led to a higher efficiency. *Siddiqui and Almitani* [34] presented an energy model of a supercritical CO_2 cycle, and resulted that at a constant turbine inlet temperature, the total efficiency of the system was proportional to the turbine inlet pressure. Ahmadi *et al*. [35] have investigated the feasibility of utilizing LNG as a heat sink for a power production layout comprised of solid oxide fuel cell, gas turbine, and organic Rankine cycle, and evaluated the designed system through the energy and exergy criteria.

In this investigation, a thermodynamic study was carried out on a solar-based transcritical CO_2 cycle. LNG was considered as its heat sink in the energy recovery unit. In addition, the cryogenic energy of LNG was utilized in the condenser and also a Stirling engine was substituted with the condenser in order to generate more electricity. Exergy assessment in addition to some other comparisons between the two proposed modes of absence and existence of the Stirling engine was also made to illustrate its advantages.

2. System Description

A schematic diagram of the solar-powered transcritical CO_2 power cycle is demonstrated in figure 1. The presented process is aimed to generate electricity based on the recovery of the cryogenic energy of LNG. The condenser of the CO_2 cycle is replaced by a Stirling engine.

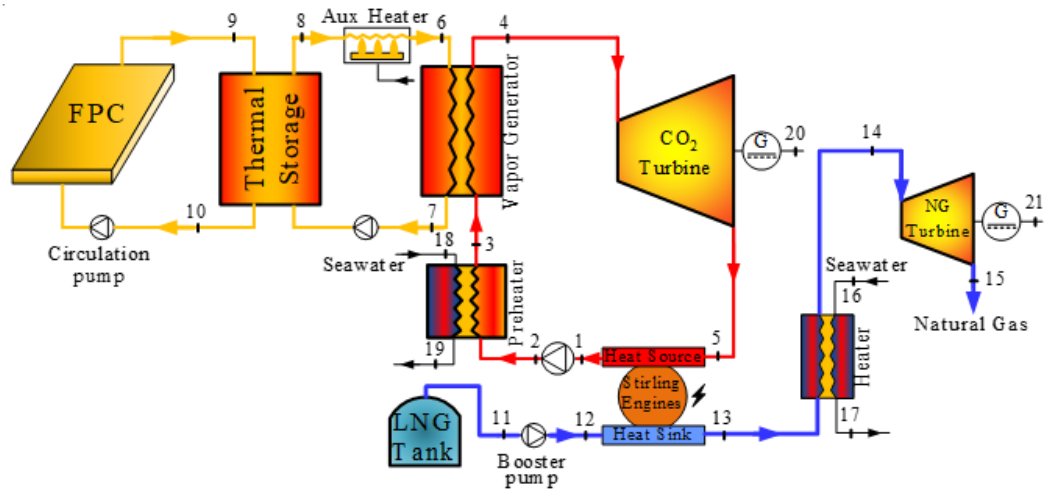

Figure 1. Schematic representation of the modeled system.

The system is composed of two major parts, the solar section of flat plate collectors (FPCs) and the power production section, respectively. The latter consists of a transcritical CO_2 cycle and an LNG unit. In the solar section, FPCs were designed to utilize solar energy. The solar thermal energy is

absorbed in FPC, and it leads to an increase in the temperature of the heat transfer fluid [36]. To surmount the intermittency of solar energy and also to provide a constant heating load, a thermal storage tank and an auxiliary heater are designed and added to the process [24]. The CO_2 transcritical power cycle consists of a vapor regenerator, a CO_2 turbine, a condenser that is here substituted by a Stirling engine, a pump, and a pre-heater. The pre-heater is used to increase the working fluid temperature before entering the vapour generator. The vapour regenerator supplied the required heat to vaporize the CO_2 flow. The mechanical work is extracted from the high-temperature CO_2 in the turbine. In order to complete the cycle, the expanded CO_2 should be condensed. Both of the used fluids in the condenser are profitably suitable for being utilized in a Stirling engine from a thermodynamics viewpoint. Therefore, replacing the condenser with a Stirling engine not only meets the required outlet condition of the condenser but also produces more electricity. Hence, the CO_2 working fluid was a heat source and LNG was a heat sink. At last, the pump augments the pressure of the liquefied CO_2 to be used in the next stages of the cycle. The LNG power cycle is used to condensate the CO_2 flow and also produce more power by recovering the energy of LNG. Thus saturated natural gas is pumped through the LNG storage tank at the ambient pressure. Moreover, its temperature is raised up in the Stirling engine when it is pumped to a specified pressure. Another heater is also provided to increase the fluid temperature to fulfill the favorable condition before it enters the NG turbine.

The following items are assumed to make the system simpler and easier to be mathematically modeled [9] :

- A 2% pressure drop in the boiler, pre-heater, and heat exchangers of the Stirling engine.
- The Kinetic and potential energies are neglected. Besides, a steady-state condition is assumed for all the processes.
- Fluids enter the pumps at the saturated condition.
- There is no heat transfer to ambient.
- The Stirling engine operates in an ideal condition.

2. System Modeling

The following equations are used, and a mathematical model is developed using the Matlab software and Refprop 8.0 to obtain the fluid properties [37].

3.1. Solar flat plate collectors and thermal storage tank

The useful heat gain rate by flat plate collectors is calculated by [38]:

$$Q_u = A_{CLT} F_R \left[S - U_L (T_i - T_{amb}) \right] \quad (1)$$

where A_{CLT} is the surface area of the solar collector, U_L is the total loss coefficient, and T denotes the temperature. F_R and S are the heat removal factor and total absorbed solar radiation, respectively, which are calculated as below [37]:

$$F_R = F'F'' \quad (2)$$

where:

$$F'' = \left(\dot{m} C_p / A_{CLT} F' U_L \right) \left[1 - \exp\left(-A_{CLT} F' U_L / \dot{m} C_p \right) \right] \quad (3)$$

$$F' = (1/U_L) \Big/ \left(W \left[1/(U_L (D + (W - D) F)) + 1/\pi D_i h_{fi} \right] \right) \quad (4)$$

$$F = \tanh\left[\sqrt{U_L / K_P \delta_P} \left(W - D/2 \right) \right] \Big/ \left(\sqrt{U_L / K_P \delta_P} \left(W - D/2 \right) \right) \quad (5)$$

$$S = I_b R_b (\tau\alpha)_b + I_d (\tau\alpha)_d \left(\frac{1 + \cos\beta}{2} \right) + \rho_g I (\tau\alpha)_g \left(\frac{1 - \cos\beta}{2} \right) \quad (6)$$

where F' denotes the collector efficiency factor and F'' indicates the flow factor. I_b is the beam radiation and I_d is the diffusion radiation. R_b denotes the ratio of the beam radiation. Kp represents the thermal conductivity and δ_P is the thickness of the plate.

Moreover, the heat transfer equation of a proper-insulated thermal storage tank is given below. It is noticeable that its temperature uniformly varies with time [39].

$$\left[(\rho V C_p)_W + (\rho V C_p)_{\mathrm{Tank}} \right] \frac{dT_{TST}}{dt} = Q_u - Q_{load} - Q_L \quad (7)$$

The following parameters are also defined as the useful heat, Q_u, load of the system, Q_{load}, and heat loss for the tank, $Q_{Loss,\ Tank}$.

$$Q_u = \dot{m}_{CLT} C_P (T_9 - T_{10}) \quad (8)$$

$$Q_{load} = \dot{m}_{load} C_P (T_8 - T_7) \quad (9)$$

$$Q_{Loss,\mathrm{Tank}} = (UA)_{\mathrm{Tank}} (T_{10} - T_{amb}) \quad (10)$$

3.2. Transcritical CO2 power cycle and LNG unit

The transcritical CO_2 cycle equations can be derived as below by applying the conservation of mass and energy principles [40]:

$$Q_{VG} = \dot{m}_{CO_2}(h_4 - h_3) \quad (11)$$

$$Q_{P-Heater} = \dot{m}_{CO_2}(h_3 - h_2) \quad (12)$$

$$W_{T,CO_2} = \dot{m}_{CO_2}(h_4 - h_5) \quad (13)$$

$$W_{P,CO_2} = \dot{m}_{CO_2}(h_1 - h_2) \quad (14)$$

$$W_{net,CO_2} = W_{P,CO_2} + W_{T,CO_2} \quad (15)$$

The rejected heat from the CO_2 working fluid enters a heat exchanger. This heat exchanger is a heat source of the Stirling engine after producing power in CO_2 turbine; $Q_{Source, StE}$ is calculated by:

$$Q_{Source,StE} = \dot{m}_{CO_2}(h_5 - h_1) \quad (16)$$

The same equation is also governed by the LNG cycle, and the other equations can be expressed as below [40]:

$$Q_{Sink,StE} = \dot{m}_{LNG}(h_{13} - h_{12}) \quad (17)$$

$$W_{P,LNG} = \dot{m}_{LNG}(h_{11} - h_{12}) \quad (18)$$

$$W_{T,NG} = \dot{m}_{LNG}(h_{14} - h_{15}) \quad (19)$$

$$Q_{Heater} = \dot{m}_{LNG}(h_{14} - h_{13}) \quad (20)$$

$$W_{net,LNG} = W_{T,NG} + W_{P,LNG} \quad (21)$$

where $Q_{sink,StE}$, $W_{p,LNG}$, $W_{T,NG}$, Q_{Heater}, and $W_{net, LNG}$ are the amount of thermal energy at the sink, the work of pump at the LNG section, the work of NG turbine, the amount of heat provided by the heater, and the total work of the LNG section, respectively.

3.3. Stirling engine

The T-S diagram of the Stirling engine is schematically demonstrated in Figure 2. In process 1-2, the piston pressurizes the fluid at a fixed temperature, and its heat is transferred to the sink (LNG section). In the following, in process 2-3, an isochoric process causes to increase the fluid temperature, and at the consequent step expands at process 3-4, and finally, drops its heat at the isochoric process 4-1.

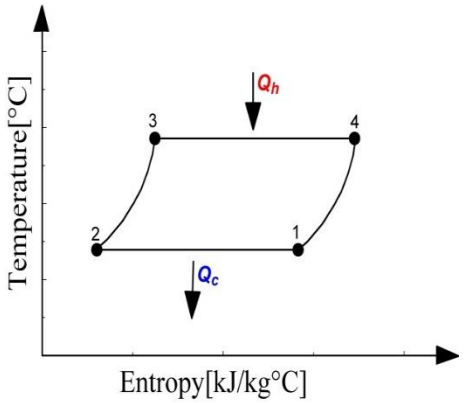

Figure 2. Stirling engine T-S diagram.

The governing equations of an ideal Stirling engine are:

$$Q_C = mRT_C \ln\left(V_{\min}/V_{\max}\right) \quad (22)$$

$$Q_h = mRT_h \ln\left(V_{\max}/V_{\min}\right) \quad (23)$$

$$W_{net,StE} = mR(T_h - T_C)\ln\left(V_{\max}/V_{\min}\right) \quad (24)$$

$$\eta_{StE} = W_{net,StE}/Q_h = \left(T_h - T_c\right)/T_h = 1-(T_C/T_h) \quad (25)$$

Equation (23) shows that the energy efficiency of the Stirling cycle is similar to its Carnot efficiency [41–45].

4. Exergy Analysis

The exergy concept is introduced as the highest achievable useful work as the result of the interaction of a system and environment to come to the equilibrium state [46, 47]. This method has a beneficial advantage, specifying the exergy destruction in each device and the flow associated with the system irreversibility [48, 49]. The exergy of streams and the exergy destruction in the components are calculated by employing the following equations:

$$ex_i = (h_i - h_0) - T_0(s_i - s_0) \quad (26)$$

$$\sum_{inlet} \dot{m}_i ex_i + Ex(Q_i) + W_i = \sum_{outlet} \dot{m}_e ex_e + Ex(Q_e) + W_e + I \quad (27)$$

Based on the exergy destruction equation, the following table demonstrates the irreversibility of each unit in the modeled system.

Table 1. Exergy destruction in equipment.

Unit	Equation	Unit	Equation
Solar radiation	$Ex_{solar} = Q_{Sun}\left(1+1/3(T_0/T_S)^4 - 4/3(T_0/T_S)\right)$*	Pre-heater	$I_{P-heater} = (Ex_{19} - Ex_{19}) - (Ex_3 - Ex_2)$
Storage tank	$I_{TST} = Ex_9 + Ex_7 - (Ex_8 + Ex_{10} + Ex_{Loss} + Ex_{Store})$	LNG pump	$I_{P.LNG} = W_{P,LNG} - (Ex_{12} - Ex_{11})$
Aux heater	$I_{Aux} = (Ex_{fuel}) - (Ex_6 - Ex_8)$	Heater	$I_{Heater} = (Ex_{16} - Ex_{17}) - (Ex_{14} - Ex_{13})$
Vapour generator	$I_{VG,CO_2} = (Ex_6 - Ex_7) - (Ex_4 - Ex_3)$	NG Turbine	$I_{T,NG} = (Ex_{14} - Ex_{15}) - W_{T,NG}$
CO_2 turbine	$I_{T,CO_2} = (Ex_4 - Ex_5) - W_{T,CO_2}$	Stirling Engines	$I_{StE} = (Ex_5 - Ex_1) - (Ex_{13} - Ex_{12}) - W_{StE}$
CO_2 pump	$I_{P,CO_2} = W_{P,CO_2} - (Ex_2 - Ex_1)$		

*The equation refers to [24].

5. Results and Discussion

A numerical investigation was performed on the novel solar-powered CO_2 transcritical cycle with the recovery of cryogenic LNG, employing the Stirling engine instead of the condenser. The required meteorological data (i.e. the irradiation, temeprature, and wind data) of Eshtehard Province's (Iran) on May 15th was used [50]. Table 2 illustrates a summary of the simulation condition in this model.

Table 2. Design parameters of the model.

Parameter	Unit	Value
Total surface of collectors	m^2	384
CO_2 turbine inlet pressure	MPa	10
CO_2 turbine inlet temperature	˚C	65
CO_2 turbine isentropic efficiency	%	70
CO_2 pump isentropic efficiency	%	80
CO_2 condensation temperature	˚C	-10
Minimum pinch temperature difference in vapour generator and condenser	˚C	10
Pressure drop in VG and pre-heater	%	2
LNG tank temperature	˚C	-161.47
LNG working pressure	MPa	6.31
LNG pump isentropic efficiency	%	70
NG turbine isentropic efficiency	%	80
NG turbine inlet temperature	˚C	10
NG turbine outlet pressure	MPa	4.00
Heater and pre-heater hot side temperature drop	˚C	20

As shown in Figure 3, which illustrates the overall performance of solar collectors and storage tank sub-systems throughout the specified day, the total absorbed radiation, and consequently, the useful heat gain significantly changes throughout the day. The solar utilization power was about zero at the periods when no required sunlight was available. On the other hand, it strongly reached a peak in mid-days (about 12 a.m.). Then as expected, it diminished to the lowest level as the sun light disappeared. It is clearly understandable that air temperature varies during hours, and it is not constant since the solar radiation values change. Therefore, to provide a fixed amount of a satisfactory heat load that meets the required demand during a day, a thermal storage tank is provided. As monitored in the figure, a smooth fall can be noticed in the temperature of water in the storage tank. Consequently, it faces a sensible rise due to absorbing heat by flat plate collectors, and then a fall after reaching the maximum condition.

The maximum state of the system was selected at 3.00 p.m., and consequently, the thermodynamic parameters, total output power, and exergy analysis in both different modes where the condenser exists and the Stirling engine was replaced, were

calculated at this base time. Accordingly, the outcomes for the indicated points demonstrated in Figure 1 are listed in Table 3. It is remarkable that the defined dead-state for performing the exergy analysis is the ambient temperature and pressure.

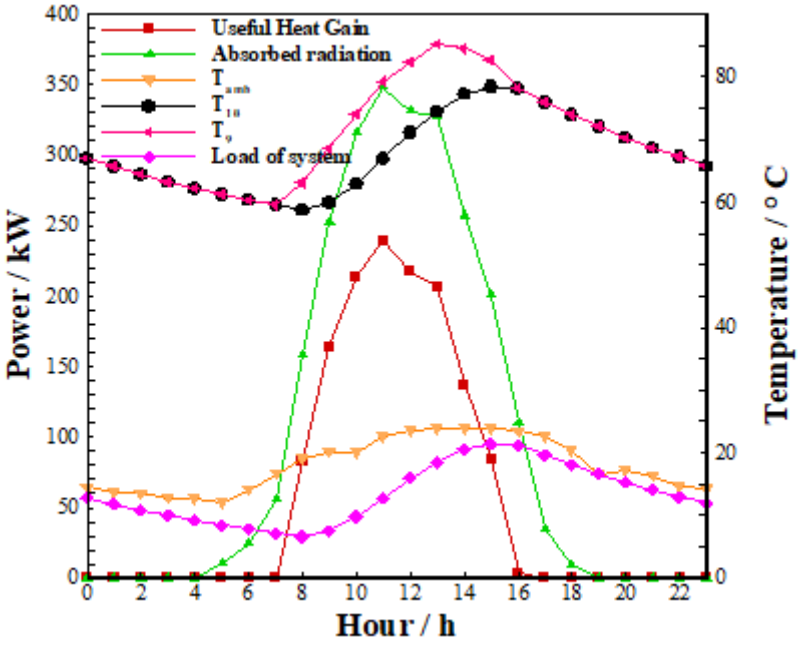

Figure 3. Overall performance of solar sub-system (daily), reprinted with permission of Elsevier [51].

Table 3. Simulation results.

State	T (˚C)	P(MPa)	Ex (kJ/kg)	$\dot{m}$ (kg/s)–in the presence of Stirling	$\dot{m}$ (kg/s)–in the presence of condenser
1	-10.000	2.649	213.637	0.520	0.520
2	-4.180	10.412	221.235	0.520	0.520
3	20.000	10.204	217.644	0.520	0.520
4	65.000	10.000	226.956	0.520	0.520
5	-9.298	2.702	185.064	0.520	0.520
6	78.335	0.101	17.867	0.800	0.800
7	50.000	0.101	4.150	0.800	0.800
8	78.335	0.101	17.867	0.800	0.800
9	82.696	0.101	20.742	4.600	4.600
10	78.051	0.101	17.867	4.600	4.600
11	-161.470	0.101	1079.966	0.173	0.212
12	-157.896	6.578	1084.710	0.173	0.212
13	-59.298	6.446	682.006	0.173	0.212
14	10.000	6.317	623.513	0.173	0.212
15	-17.860	4.000	566.438	0.173	0.212
16	25.000	0.101	0.000	0.506	0.623
17	5.000	0.099	2.943	0.506	0.623
18	25.000	0.101	0.000	0.347	0.347
19	5.000	0.099	2.943	0.347	0.347

It can be seen that in the same condition, in the system containing Stirling engines, the mass flow rate of the LNG cycle is decreased by 0.039 (kg/s) because of the lower heat rejection by engines to the LNG cycle as their heat sink. Eventually, the LNG mass flow rate, and consequently, the flow rate of cooling water in the heater are lowered. Therefore, the required area of the heat exchanger is decreased in the same thermodynamic condition. Furthermore, the exergy flow encompassing input, output, and destruction for the system based on exergy equations are presented in Table 4 in the attendance of either Stirling or condenser. The table shows that near half of the inlet exergy to the system consists of solar exergy and LNG tank flow, secondly. This useful gained work by the system mostly destructs the flat plate collectors by 46.31% with cycle including Stirling and 41.55% in the other. The condenser is in the second place of exergy destruction by about 17%, while this value for the system with Stirling reduces to 8.85%, which is approximately more than half. Meanwhile, this noticeable power is added to useful output exergy as Stirling engine power output, which is equal to 21.482 kW. This value is much more than the summation of the total output power of both the LNG cycle and the CO_2 cycle being 9.55 and 3.85 kW, respectively. As a result, the exergy destruction due to the attendance of Stirling engines is 33.25 kW, which is 37.53 kW less than the amount of exergy destruction by the condenser. Based on the results obtained, it can be concluded that the exergy flow of stream No. 15 is proportional to the mass flow rate of LNG.

Table 4. Exergy flow through the system analysis.

Position		Value (kW) with Stirling	Percentage with Stirling (%)	Value (kW) with condenser	Percentage with condenser (%)
Exergy input	Solar	187.121	50.059	187.121	50.059
	LNG tank	186.681	49.941	229.72	55.110
Exergy destruction	Flat plate collectors	173.899	46.317	173.899	41.554
	Thermal storage tank	3.898	1.038	3.898	0.931
	Vapour generator	6.126	1.632	6.126	1.464
	CO_2 turbine	7.116	1.895	7.116	1.700
	CO_2 pump	1.184	0.315	1.184	0.283
	Pre-heater	0.846	0.225	0.846	0.202
	Stirling engines/Condenser	33.254	8.857	70.784	16.914
	Booster pump	2.951	0.786	3.631	0.868
	Heater	8.621	2.296	10.608	2.535
	NG turbine	2.244	0.598	2.761	0.660
Exergy output	Stream No.19	1.023	0.273	1.023	0.244
	Stream No.17	1.490	0.397	1.834	0.438
	Stream No.15	97.914	26.079	120.487	28.791
	CO_2 power production	9.553	2.544	9.553	2.283
	NG power production	3.851	1.026	4.738	1.132
	Stirling engine work	21.482	5.722	0.000	0.000

Figure 4 depicts the variation in the total output power and flow rate of LNG both in the absence and in the presence of the Stirling. At the times without any an efficient sunlight during the day, the heater provides a stable load satisfying pinch in the vapour generator. Thus during the first 11 hours, the stable output power is obvious, while the output power increases as the solar radiation rises. It can be monitored that the output power in the system with Stirling engines is hugely increased by about

15 kW in the off-peak times and more than 20 kW in the peak times. Any changes in the load of the system bring about fluctuations in the CO_2 flow rate of the power cycle, which leads to the variation in the LNG mass flow rate in the same thermodynamic conditions. Figure 4 also shows this variation in the LNG mass flow rate, which is decreased due to the use of Stirling engines instead of the condenser. Though this would decrease the net power output of the natural gas turbine (less than 1 kW, based on Table 4), the overall net output power increases.

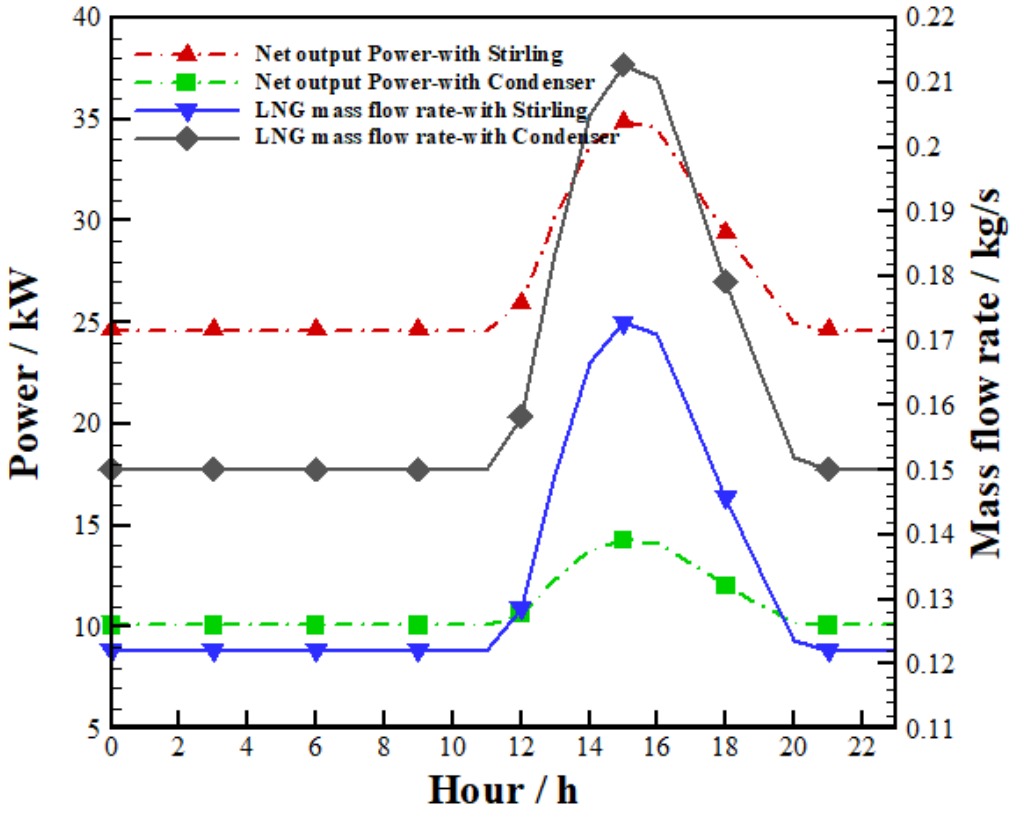

Figure 4. Total power of the system and LNG mass flow rate.

5. Conclusion

In this investigation, a novel solar-powered CO_2 transcritical power cycle with the recovery of cryogenic LNG was studied, and the feasibility of replacing a typical condenser by a Stirling engine was discussed. In order to examine the performance of the presented system, the exergy analysis was performed, and the results obtained were compared for both defined statuses to monitor the possible benefits of integrating a Stirling engine to the CO_2 power cycle as follows:

- Integration of the Stirling engine reduced the mass flow rate of the LNG unit. It should be noted that a low flow rate in the LNG section leads to reduce the flow rate of cooling water.
- The required area of the heat exchanger was significantly decreased.
- Based on the exergy analysis, the solar unit was the most exergy destructive section. The solar collectors in both cases were the 1st rank in exergy destruction rate, 46.3% in the presence of the Stirling engine, and 41.5% in the presence of a typical condenser unit.
- Focusing on the distinction on two introduced cycle stated that the typical condenser exergy destruction rate was 17%, while this amount was decreased to 8.85% by replacing a Stirling engine.
- Utilizing the Stirling engine lowered the output power of the NG turbine, meanwhile the overall output power was significantly increased since the Stirling engine produced 21.48 kW power by itself.

Nomenclature

A	Area [m^2]
C_p	Specific heat capacity [J/kg K]
D	Diameter [m]
Ex	Exergy [kW]
Ex	Specific exergy [kJ/kg]
F_R	Collector heat removal factor
F'	Collector efficiency factor
F''	Flow factor
FPC	Flat plate collector

h_{fi}	Heat transfer coefficient inside the tubes [W/m^{2}K]
I	Radiation [W/m^2]; exergy destruction [kW]
K	Thermal conductivity [W/mK]
$\dot{m}$	Mass flow rate [kg/s]
NG	Natural gas
Q	Heat [kW]
R_b	Beam radiation tilt factor
R	Universal gas constant [J mol^{-1} K^{-1}]
S	Specific entropy [kJ/kg]; total absorbed solar radiation [W/m^2]
T	Temperature [˚C; K]
U	Heat transfer coefficient [W/m^2 K]
VG	Vapour generator
V	Volume [m^3]
W	Tube spacing [m]; power [kW]

Greek

β	Slope of collector [degree]
δ	Declination angle [degree]; thickness [m]
π	Pi number
ρ	Density [kg/m^3]

Subscript

amb	Ambient
Aux	Auxiliary
b	Beam
c	Cold
CLT	Collector
d	Diffuse
g	Ground
h	Hot
i	Inner; inlet
L	Loss
P	Absorber plate; pump
TST	Thermal storage tank
StE	Stirling engine
T	Turbine
U	Useful
0	Dead state

References

[1] Haghighi Bardineh Y, Mohamadian F, Ahmadi MH, Akbarianrad N. Medical and dental applications of renewable energy systems. Int J Low-Carbon Technol 2018:1–7. doi:10.1093/ijlct/cty040.

[2] Rezaei MH, Sadeghzadeh M, Alhuyi Nazari M, Ahmadi MH, Astaraei FR. Applying GMDH artificial neural network in modeling CO2 emissions in four nordic countries. Int J Low-Carbon Technol 2018:1–6. doi:10.1093/ijlct/cty026.

[3] Dincer I, Hussain MM. Energy and exergy use in the industrial sector 2003;217:481–92.

[4] Ahmadi MH, Ghazvini M, Sadeghzadeh M, Alhuyi Nazari M, Kumar R, Naeimi A, et al. Solar power technology for electricity generation: A critical review. Energy Sci Eng 2018:1–22. doi:10.1002/ese3.239.

[5] Mohammadi A, Ahmadi MH, Bidi M, Ghazvini M, Ming T. Exergy and economic analyses of replacing feedwater heaters in a Rankine cycle with parabolic trough collectors. Energy Reports 2018;4:243–51. doi:10.1016/J.EGYR.2018.03.001.

[6] Sadeghzadeh M, Ahmadi MH, Kahani M, Sakhaeinia H, Chaji H, Chen L. Smart modeling by using artificial intelligent techniques on thermal performance of flat-plate solar collector using nanofluid. Energy Sci Eng 2019;0. doi:10.1002/ese3.381.

[7] Ghorbani B, Mehrpooya M, Sadeghzadeh M. Developing a tri-generation system of power, heating, and freshwater (for an industrial town) by using solar flat plate collectors, multi-stage desalination unit, and Kalina power generation cycle. Energy Convers Manag 2018;165:113–26. doi:10.1016/J.ENCONMAN.2018.03.040.

[8] Chen H, Goswami DY, Stefanakos EK. A review of thermodynamic cycles and working fluids for the conversion of low-grade heat. Renew Sustain Energy Rev 2010;14:3059–67. doi:10.1016/J.RSER.2010.07.006.

[9] Crespi F, Gavagnin G, Sánchez D, Martínez GS. Supercritical carbon dioxide cycles for power generation: A review. Appl Energy 2017;195:152–83. doi:10.1016/j.apenergy.2017.02.048.

[10] Hernández-Jiménez F, Soria-Verdugo A, Acosta-Iborra A, Santana D. Exergy recovery from solar heated particles to supercritical CO2. Appl Therm Eng 2019;146:469–81. doi:10.1016/j.applthermaleng.2018.10.009.

[11] Ahmadi MH, Mehrpooya M, Abbasi S, Pourfayaz F, Bruno JC. Thermo-economic analysis and multi-objective optimization of a transcritical CO2 power cycle driven by solar energy and LNG cold recovery. Therm Sci Eng Prog 2017;4:185–96. doi:10.1016/J.TSEP.2017.10.004.

[12] Chen Y, Lundqvist P, Johansson A, Platell P. A comparative study of the carbon dioxide transcritical power cycle compared with an organic rankine cycle with R123 as working fluid in waste heat recovery. Appl Therm Eng 2006;26:2142–7. doi:10.1016/J.APPLTHERMALENG.2006.04.009.

[13] Chen Y, Pridasawas W, Lundqvist P. Dynamic simulation of a solar-driven carbon dioxide transcritical power system for small scale combined heat and power production. Sol Energy 2010;84:1103–10. doi:10.1016/J.SOLENER.2010.03.006.

[14] Cayer E, Galanis N, Desilets M, Nesreddine H, Roy P. Analysis of a carbon dioxide transcritical power cycle using a low temperature source. Appl Energy 2009;86:1055–63. doi:10.1016/J.APENERGY.2008.09.018.

[15] Wang J, Sun Z, Dai Y, Ma S. Parametric optimization design for supercritical CO2 power cycle using genetic algorithm and artificial neural network. Appl Energy 2010;87:1317–24. doi:10.1016/J.APENERGY.2009.07.017.

[16] Zhang XR, Yamaguchi H, Uneno D, Fujima K, Enomoto M, Sawada N. Analysis of a novel solar energy-powered Rankine cycle for combined power and heat generation using supercritical carbon dioxide. Renew Energy 2006;31:1839–54. doi:10.1016/J.RENENE.2005.09.024.

[17] Zhang XR, Yamaguchi H, Fujima K, Enomoto M, Sawada N. Theoretical analysis of a thermodynamic cycle for power and heat production using supercritical carbon dioxide. Energy 2007;32:591–9. doi:10.1016/J.ENERGY.2006.07.016.

[18] Zhang XR, Yamaguchi H, Uneno D. Thermodynamic analysis of the CO2-based Rankine cycle powered by solar energy. Int J Energy Res 2007;31:1414–24. doi:10.1002/er.1304.

[19] Yamaguchi H, Zhang XR, Fujima K, Enomoto M, Sawada N. Solar energy powered Rankine cycle using supercritical CO2. Appl Therm Eng 2006;26:2345–54. doi:10.1016/J.APPLTHERMALENG.2006.02.029.

[20] Zhang XR, Yamaguchi H, Fujima K, Enomoto M, Sawada N. Study of solar energy powered transcritical cycle using supercritical carbon dioxide. Int J Energy Res 2006;30:1117–29. doi:10.1002/er.1201.

[21] Zhang X-R, Yamaguchi H, Uneno D. Experimental study on the performance of solar Rankine system using supercritical CO2. Renew Energy 2007;32:2617–28. doi:10.1016/J.RENENE.2007.01.003.

[22] Niu X-D, Yamaguchi H, Zhang X-R, Iwamoto Y, Hashitani N. Experimental study of heat transfer characteristics of supercritical CO2 fluid in collectors of solar Rankine cycle system. Appl Therm Eng 2011;31:1279–85. doi:10.1016/J.APPLTHERMALENG.2010.12.034.

[23] Lin W, Huang M, He H, Gu A. A Transcritical CO2 Rankine Cycle With LNG Cold Energy Utilization and Liquefaction of CO2 in Gas Turbine Exhaust. J Energy Resour Technol 2009;131:42201–5.

[24] Song Y, Wang J, Dai Y, Zhou E. Thermodynamic analysis of a transcritical CO2 power cycle driven by solar energy with liquified natural gas as its heat sink. Appl Energy 2012;92:194–203. doi:10.1016/J.APENERGY.2011.10.021.

[25] Zhang N, Lior N. A novel near-zero CO2 emission thermal cycle with LNG cryogenic exergy utilization. Energy 2006;31:1666–79. doi:10.1016/J.ENERGY.2005.05.006.

[26] Liu M, Lior N, Zhang N, Han W. Thermoeconomic analysis of a novel zero-CO2-emission high-efficiency power cycle using LNG coldness. Energy Convers Manag 2009;50:2768–81. doi:10.1016/J.ENCONMAN.2009.06.033.

[27] Dong H, Zhao L, Zhang S, Wang A, Cai J. Using cryogenic exergy of liquefied natural gas for electricity production with the Stirling cycle. Energy 2013;63:10–8. doi:10.1016/J.ENERGY.2013.10.063.

[28] Szczygieł I, Stanek W, Szargut J. Application of the Stirling engine driven with cryogenic exergy of LNG (liquefied natural gas) for the production of electricity. Energy 2016;105:25–31. doi:10.1016/J.ENERGY.2015.08.112.

[29] Szargut J, Szczygiel I. Utilization of the cryogenic exergy of liquid natural gas (LNG) for the production of electricity. Energy 2009;34:827–37. doi:10.1016/J.ENERGY.2009.02.015.

[30] Ge YT, Li L, Luo X, Tassou SA. Performance evaluation of a low-grade power generation system with CO2transcritical power cycles. Appl Energy 2018;227:220–30. doi:10.1016/j.apenergy.2017.07.086.

[31] Sarmiento C, Cardemil JM, Díaz AJ, Barraza R. Parametrized analysis of a carbon dioxide transcritical Rankine cycle driven by solar energy. Appl Therm Eng 2018;140:580–92. doi:10.1016/j.applthermaleng.2018.04.097.

[32] AlZahrani AA, Dincer I. Thermodynamic analysis of an integrated transcritical carbon dioxide power cycle for concentrated solar power systems. Sol Energy 2018;170:557–67. doi:10.1016/j.solener.2018.05.071.

[33] Naseri A, Bidi M, Ahmadi M, Saidur R. Exergy analysis of a hydrogen and water production process by a solar-driven transcritical CO2 power cycle with Stirling engine. J Clean Prod 2017;158:165–81. doi:10.1016/J.JCLEPRO.2017.05.005.

[34] Siddiqui M, Almitani K. Energy Analysis of the S-CO2 Brayton Cycle with Improved Heat Regeneration. Processes 2018;7:3. doi:10.3390/pr7010003.

[35] Ahmadi MH, Sadaghiani MS, Pourfayaz F, Ghazvini M, Mahian O, Mehrpooya M, et al. Energy and exergy analyses of a solid oxide fuel cell-gas turbine-organic rankine cycle power plant with liquefied natural gas as heat sink. Entropy 2018;20:1–22. doi:10.3390/e20070484.

[36] Bensaci C, Labed A, Universit MZ, Moummi A. Numerical study of natural convection in an inclined enclosure : application to flat plate solar collectors 2017. doi:10.18280/mmep.040101.

[37] Lemmon WE, Huber LM MO. NIST reference fluid thermodynamic and transport properties. 2010. doi:REFPROP.

[38] Sukhatme SP. Solar energy : principles of thermal collection and storage 1997.

[39] Kalogirou SA. Solar Energy Engineering: Processes and Systems. 2009. doi:10.1016/B978-0-12-374501-9.00014-5.

[40] Xia G, Sun Q, Cao X, Wang J, Yu Y, Wang L. Thermodynamic analysis and optimization of a solar-powered transcritical CO2 (carbon dioxide) power cycle for reverse osmosis desalination based on the recovery of cryogenic energy of LNG (liquefied natural gas). Energy 2014;66:643–53. doi:10.1016/J.ENERGY.2013.12.029.

[41] Kongtragool B, Wongwises S. Thermodynamic analysis of a Stirling engine including dead volumes of hot space, cold space and regenerator. Renew Energy 2006;31:345–59. doi:10.1016/J.RENENE.2005.03.012.

[42] Mahmoodi mostafa. Analysis and optimization of beta-type Stirling engine taking into account the non-ideal regenerator thermal and hydraulic losses effects. Modares Mech Eng 2011;12.

[43] Possamai DG, Tapia GIM. Thermodynamics analysis of Stirling Engine 2011.

[44] Puech P, Tishkova V. Thermodynamic analysis of a Stirling engine including regenerator dead volume. Renew Energy 2011;36:872–8. doi:10.1016/J.RENENE.2010.07.013.

[45] Thombare DG, Verma SK. Technological development in the Stirling cycle engines. Renew Sustain Energy Rev 2008;12:1–38. doi:10.1016/J.RSER.2006.07.001.

[46] Gulotta TM, Guarino F, Mistretta M, Cellura M, Lorenzini G. Introducing exergy analysis in life cycle assessment: A case study. Math Model Eng Probl 2018;5:139–45. doi:10.18280/mmep.050302.

[47] Karimi M, Ghorbanian K, Gholamrezaei M. Energy and exergy analyses of an integrated gas turbine thermoacoustic engine. Proc Inst Mech Eng Part A J Power Energy 2011;225:389–402. doi:10.1177/0957650911399017.

[48] Dinçer I, Rosen M (Marc A. EXERGY : Energy, Environment and Sustainable Development. Elsevier Science; 2012.

[49] Chen CK, Su YF. Application of exergy method to an irreversible inter-cooled refrigeration cycle. Proc Inst Mech Eng Part A J Power Energy 2005;219:661–8. doi:10.1243/095765005X69242.

[50] (SANA) R energy organization of I. Database for solar irradiation n.d. www.suna.org.ir.

[51] Naseri A, Bidi M, Ahmadi MH. Thermodynamic and exergy analysis of a hydrogen and permeate water production process by a solar-driven transcritical CO2 power cycle with liquefied natural gas heat sink. Renew Energy 2017;113:1215–28. doi:10.1016/J.RENENE.2017.06.082.